

Microrobots in food science and technology

Received: 6 March 2024

Accepted: 15 October 2025

Published online: 3 December 2025

 Check for updates

Roberto Maria-Hormigos¹, Carmen C. Mayorga-Martinez^{1,2,3} & Martin Pumera^{1,2,4,5} 

The global food supply chain is highly susceptible to spoilage and contamination risks, posing severe health hazards to consumers. This creates the need for preservation and safety-monitoring methods to reduce the exposure of both industries and consumers to these risks. Recent innovations using functional materials to construct nano- and microrobots of different shapes and sizes show substantial improvements in optimizing various food processes. Here we review the benefits of applying autonomous functional microrobotics to food science and technology, focusing on applications in food safety control, preservation and processing. We identify current limitations specific to each application and general constraints that must be overcome to transition from proof of concept to real-world implementation in the food industry.

In the food industry, production and handling are centralized in facilities that span the supply chain—from farms and processing plants to storage warehouses and supermarkets. While centralization decreases the cost of production, transport and manufacturing, there is a persisting risk of food spoilage and contamination throughout the supply chain^{1–9}. To prevent this, faster and safer food processing and *in situ* contaminant elimination are required^{10–12}. Nano- and micromaterials have been used in the food industry as additives, preservatives and sensors for poison detection^{13–16}. However, there is a need to improve and automate food production processes. One potential solution to the challenges in food safety and manufacturing is the development of miniature moving platforms—autonomous, self-propelled microrobots that can enhance food chemistry reaction kinetics, capture bacteria or speed up processes, and that can be automatically controlled during food processing.

Self-moving microrobots are small devices at the milli-, micro- or nanoscale that can be propelled autonomously by chemicals in the environment (for example, glucose, urea or hydrogen peroxide) or by the influence of an external source, such as light, ultrasound waves or magnetic fields^{17–20}. For clarity, as micrometre-scale robots are most commonly used in food-related applications, and millimetre- or nanometre-scale versions are used only rarely, we use the term ‘microrobot’ throughout this Review, except when a more precise size specification is required.

These micro- and nanodevices can move autonomously in the aqueous environment and, when properly functionalized on the surface, can perform various tasks, such as capturing and removing or destroying pathogens, transporting and delivering chemicals, or catalytically accelerating (bio)chemical conversion²¹. These micro- and nanorobots can be designed to follow chemical gradients, light or a magnetic field, and to move in swarms, enhancing their efficiency (Fig. 1, left). This promising microrobotic technology has been used for biomedical and environmental applications and in the food-processing industry^{22–27}. In this Review, we explore how microrobots can detect food contaminants—enhancing food safety control while reducing analysis time and minimizing the need for extensive sample treatments. We describe how microrobots can aid food preservation by removing pathogens and contaminants. We also discuss using these microrobots for food processing and the challenges and future prospects of micro- and nanorobotic technology in the food industry.

Micro- and nanorobots for food safety control

In the context of food safety and processing, a central challenge in the development of functional, self-propelled microparticles or nanoparticles (NPs) (referred to herein as micro- or nanorobots) is the integration of key design elements that enable autonomous operation. These include a motorized component to generate propulsion and drive motion; functional surface layers that enable interaction

¹Future Energy and Innovation Laboratory, Central European Institute of Technology, Brno University of Technology (CEITEC-BUT), Brno, Czech Republic. ²Advanced Nanorobots and Multiscale Robotics Lab, Faculty of Electrical Engineering and Computer Science, VSB – Technical University of Ostrava, Ostrava, Czech Republic. ³School of Biomedical Engineering, Peruvian University of Applied Sciences (UPC), Prolongación Primavera, Lima, Peru. ⁴Department of Medical Research, China Medical University Hospital, China Medical University, Taichung, Taiwan. ⁵Department of Chemical and Biomolecular Engineering, Yonsei University, Seoul, Korea.  e-mail: martin.pumera@ceitec.vutbr.cz

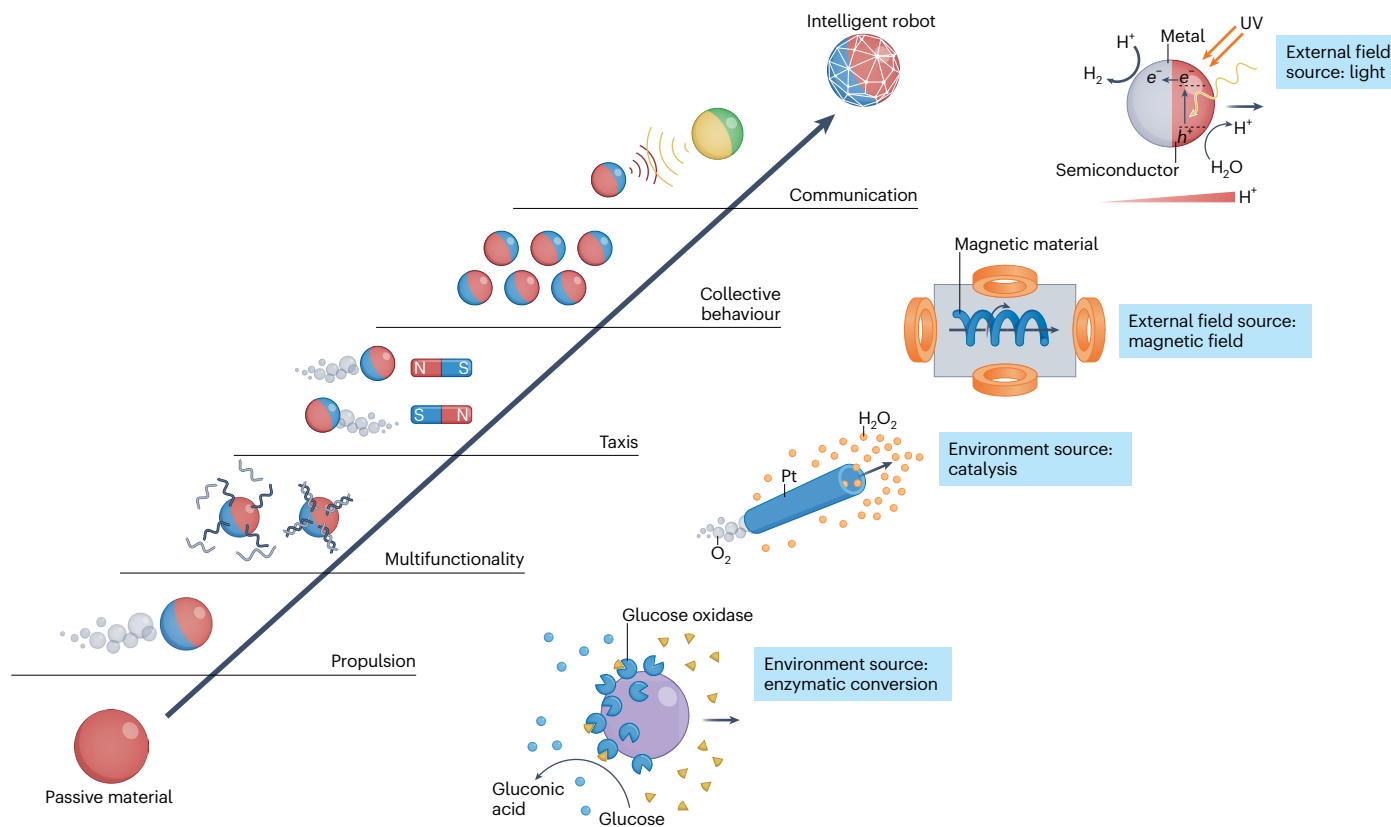


Fig. 1 | Schematics of microrobot functionalities and built-in physical intelligence. Left: evolution of micro- and/or nanomaterials from passive material to intelligent microrobot through distinct, stepwise upgrades: step 0, passive material; step 1, propulsion, that is, the autonomous or external field-induced motion (see right panel); step 2, functionality, integrating task-oriented features that meet targeted application needs; step 3, taxis, enabling navigation in response to environmental cues such as chemical (chemotaxis), light (phototaxis) or magnetic (magnetotaxis) gradients and fields; step 4, collective behaviour, fostering cooperative swarm actions to

boost efficiency or tackle tasks no single unit could manage alone; step 5, communication, allowing neighbouring robots to coordinate and synchronize their activities; and step 6, materials intelligence of a programmable responsive microrobot. Size ranges are typically 1–100 µm for microrobots and below 1 µm for nanorobots. Right: different modes of propulsion of micro- or nanorobots: (1) environment sources, such as enzymatic conversion of substrate or catalysis; or (2) external field sources, such as magnetic field or light. The key to propulsion here is the asymmetric release of reaction products or an asymmetric external field. Figure adapted with permission from ref. 25, Springer Nature Limited.

with the surrounding environment, capturing, releasing or removing specific materials or chemicals in response to programmed chemical cues; and embedded navigation mechanisms that allow the particles to respond to external stimuli such as light, chemical gradients or magnetic fields, thereby guiding their directional movement. When needed, microrobots can be designed to move in swarms and show materials intelligence^{28,29} (Fig. 1, left). For food safety and processing tasks, micro- and nanorobots are typically built as hybrids that blend structural frameworks with functional layers^{30,31}. Various materials can be used to construct the basic body of the microrobot, enabling propulsion through the catalytic decomposition of fuels³⁰ or reactive body materials³², or by responding to magnetic fields^{33,34} or ultrasound waves^{35,36} (Fig. 1, right), while also providing the structural strength needed for operation. In addition to inorganic materials, the micro- or nanorobots can be constructed from biological materials such as cells, bacteria, sporopollenin particles or protein aggregates, which can later be decorated with additional functional elements^{37–39}. These biomaterial cores of microrobots are often decorated with metal oxides—such as TiO₂, ZnO, Fe₃O₄, MnO₂ and haematite—that add photocatalytic activity, catalytic activity or, in some cases, magnetic properties. This surface functionalization can be extended to enzymes (used for either propulsion or catalytic breakdown of chemicals), antibodies or aptamers. Materials such as metal–organic frameworks and two-dimensional sheets (for example, MoS₂, MXenes and graphitic C₃N₄) provide a large surface area for chemical cargo loading or toxin adsorption, enabling

point-and-act functionality⁴⁰. The use of such materials often results in a layered architecture in which each material contributes to a specific mechanical, catalytic or biological function, together endowing the tiny robots with autonomous motion and task-specific intelligence^{41,42}.

The motion of microrobots boosts the intermixing of chemicals within food matrices, thereby accelerating the degradation of harmful substances, optimizing extraction rates and increasing the frequency of detection events^{43–46}. These screening methodologies are ideal for food evaluation after processing and before food stock reaches the market. Moreover, the microrobots’ motion improves reaction rates compared with conventional biosensors by inducing micromixing through their propulsion, thereby enhancing mass transfer^{47,48}. The surfaces of these microrobots can be tailored with bespoke receptors, enabling them to perform targeted and selective analyses crucial for food safety control. This section reviews how microrobots identify and quantify contaminants and toxins in food products.

Microrobots have been pivotal in detecting, breaking down and removing toxic compounds from foodstuffs. For example, the catalytic reactions induced by microrobots during their movement can result in localized pH variations in the surrounding medium. These pH variations are instrumental in developing sensing strategies^{47,48}. Specifically, microrobots have been developed to detect diphenyl phthalate (DPP) in food samples⁴⁷. These microrobots are composed of magnesium or gold particles and are propelled in water by producing bubbles and hydroxyl ions through magnesium decomposition. Hydrogen

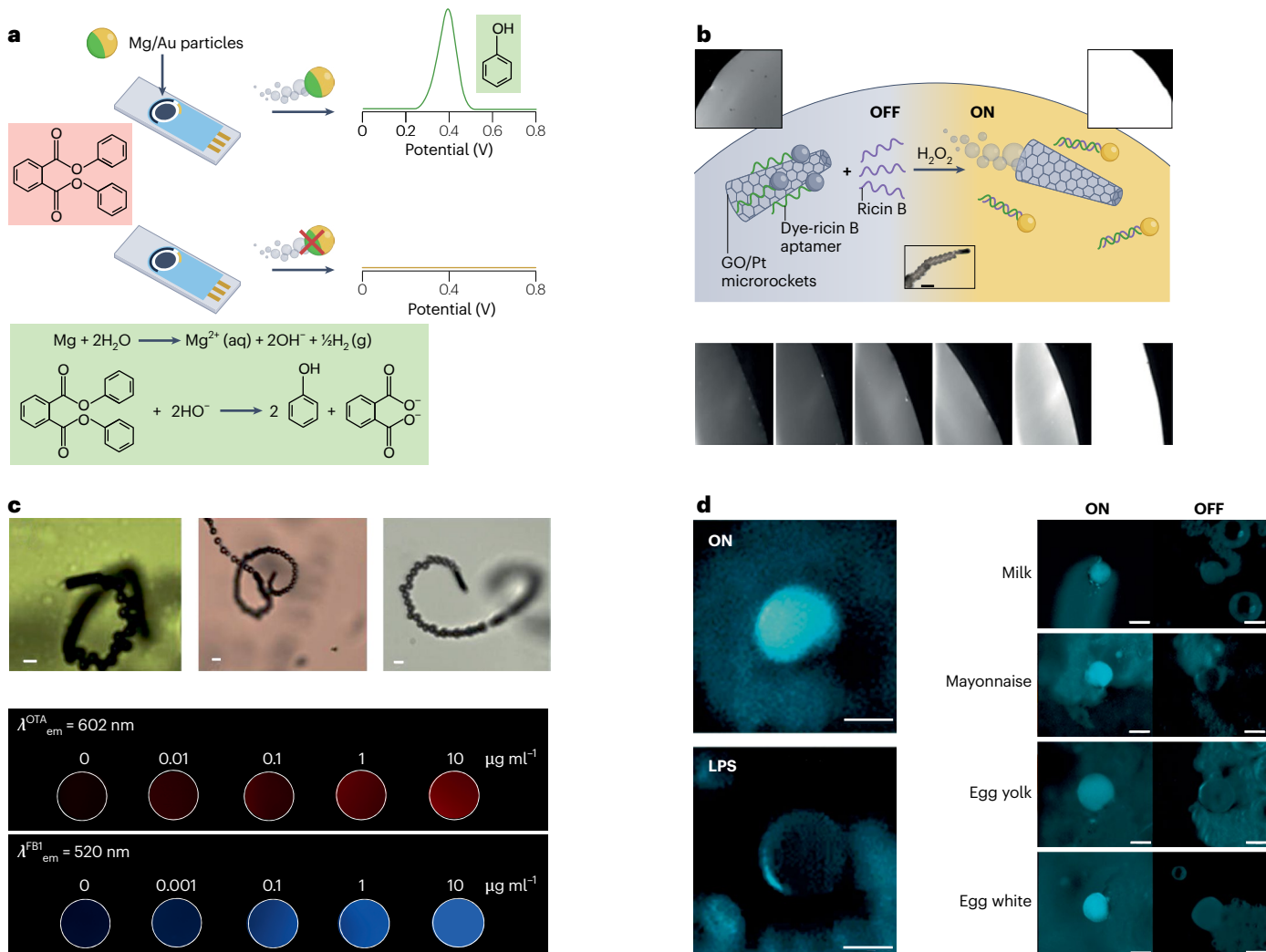


Fig. 2 | Self-propelled microrobots for food safety control applications. **a**, Scheme of the Mg/Au spherical microrobot-based strategy and the chemical reaction involved in DPP-assisted degradation and/or detection by the microrobots. The microrobot is propelled by the reaction of magnesium with water. **b**, Scheme of the off-on fluorescence detection strategy for ricin B toxin using aptamer-modified graphene/platinum tubular microrobots. Fluorescence images in the bottom row show signal intensity corresponding to ricin B concentration from $100 \mu\text{g ml}^{-1}$ to $10 \mu\text{g ml}^{-1}$. The three insets show the 'OFF' fluorescence state after aptamer incubation with the micromotors (left); a swimming microrobot in the presence of ricin B toxin in a $1\% \text{ H}_2\text{O}_2$ solution (middle); and the 'ON' fluorescence state following detection of $10 \mu\text{g ml}^{-1}$ ricin B. Scale bar, $10 \mu\text{m}$. **c**, Top: graphene/platinum tubular microrobots swimming

in different samples, such as CRM (left), beer (middle) and wine (right). Bottom: simultaneous detection of the mycotoxins OTA or FB1 by these graphene/platinum microrobots. The red and blue scales are proportional to the emission intensity of OTA and FB1 aptamers, respectively. Scale bars, $10 \mu\text{m}$. **d**, Self-propelled GQD-based microrobots for the detection of LPS from *S. enterica*. Left: fluorescence optical images show a microrobot before (on) and after (off) LPS addition. Right: LPS fluorescence detection on food samples (milk, mayonnaise, egg yolk and egg white) contaminated with LPS from *S. enterica* using self-propelled microrobots. Scale bars, $20 \mu\text{m}$. λ_{em} , emission wavelength. Panels adapted with permission from: **a**, ref. 47, American Chemical Society; **b**, ref. 51 (<https://pubs.acs.org/doi/10.1021/acssensors.5b00300>), American Chemical Society; **c**, ref. 54, American Chemical Society; **d**, ref. 57, American Chemical Society.

bubbles propel the robots, while hydroxyl ions increase the pH and hydrolyse the DPP pesticide into phenol, which can be electrochemically detected using a portable electrochemical system (Fig. 2a). In addition, the self-propelled movement of microrobots increases the rate of DPP degradation to phenol and enhances phenol's mass transfer to the electrode surface, enabling its detection in milk and whisky with almost 100% accuracy.

Manganese and iron oxide microrobots are used to reduce the time for arsenic extraction from rice samples⁴⁹. Manganese-based catalytic microrobots produce many hydroxyl radicals and oxygen bubbles during their propulsion by hydrogen peroxide decomposition. Owing to this, hydroxyl radicals produced by MnFe₂O₄ microrobots accelerate rice digestion, reducing arsenic extraction from several hours using static microparticles to less than 1.5 hours using moving microrobots⁴⁹.

This microrobot-based method was validated using a certified reference material (CRM) and showed a high accuracy of 88%.

Attaining high selectivity is crucial for conducting precise food analyses. In recent years, aptamers have emerged as powerful and selective tools for analytical assessments⁵⁰. Their robustness gives them an advantage over conventional biorecognition elements, such as antibodies, particularly when used to functionalize tubular catalytic microrobots with fluorescence-tagged aptamers. This approach has been successfully applied to detect toxins and mycotoxins in beverage samples (Fig. 2b). In this case, the microrobots were modified by a fluorescence-tagged aptamer, which had specific affinity for the toxin (ricin B). In the absence of the toxin, the microrobot in the sweeping solution has the aptamer bound to its surface and the fluorescence tag is quenched (fluorescence is in the 'off' state) by the microrobot's

surface π - π interactions. This sensing scheme is based on ‘off-on’ fluorescence switching. When the target toxin is present, binding of the toxin to the aptamer causes a conformational change that removes the quenching effect, thereby switching the fluorescence ‘on’ and signalling the presence of the toxin. This technique provides a highly selective and sensitive method for monitoring food safety⁵¹. The microrobots are engineered in a dual-layer structure, in which an inner catalytic platinum layer propels the microrobots, while an outer layer of reduced graphene oxide (GO) serves as a fluorescence quencher.

Further advances have been introduced by incorporating a magnetic layer within the microrobots’ structure to facilitate their magnetic manipulation. The utility of these microrobots has been extended to detecting the mycotoxins ochratoxin A (OTA) and fumonisins B1 (FB1), showing the versatile potential of microrobot design in contaminant detection⁵². The inner catalytic layer based on Pt NPs showed higher microrobot propulsion speed and, therefore, greater intermixing capabilities than conventional Pt catalytic layers⁵³. Incorporating an intermediate nickel magnetic layer has improved the control and manoeuvrability of these devices in liquid media. This magnetic responsiveness allows for precise positioning and halting of the microrobots, resulting in a faster assay process that takes 2 minutes. This advancement has paved the way for real-time fluorescence quenching of specific, unbound, tagged aptamers interacting with the mycotoxins OTA or FB1. The microrobots’ motion enhances aptamer binding on their surfaces, enabling *in situ* detection of these mycotoxins through real-time fluorescence quenching. Leveraging this principle, this sensing technique has been extended to simultaneously detect OTA and FB1 in a range of sample matrices, including CRMs, beer and wine in a multiplexed assay format⁵⁴ (Fig. 2c, top). The rapid 2-minute assay enables the simultaneous detection of both mycotoxins using distinct fluorescent dyes attached to the specific aptamers with different excitation and emission wavelengths (as shown in Fig. 2c, bottom). Mycotoxin analysis based on microrobot biosensing results in highly sensitive assays (at the ng ml⁻¹ scale) and accuracy comparable to CRM values (96–98%). Such findings underscore the critical role of miniaturized robotic surfaces and their functionalization in devising analytical methods for food safety monitoring.

Recently developed carbon nanomaterials, such as carbon quantum dots (CQDs) and graphene quantum dots (GQDs), have garnered attention in bioimaging due to their intrinsic fluorescence properties. The fluorescence of GQDs is particularly responsive to changes in their chemical and physical surroundings, rendering them exceptionally well suited for biosensing applications. Their environmental sensitivity positions them as promising candidates for the development of advanced biosensors⁵⁵. In this context, magneto-catalytic GQD Janus microrobots have been developed for bacterial endotoxin detection^{56,57}. Endotoxins, also known as lipopolysaccharides (LPSs), are components found in the cell walls of Gram-negative bacteria. These toxins can be released into the surrounding environment through bacterial activity, thereby serving as indicators of bacterial contamination in food samples. The sensing approach used Janus microrobots functionalized with *para*-aminobenzoic acid GQDs, whose fluorescence is dynamically quenched upon interaction with LPSs. This quenching occurs due to the specific binding of *para*-aminobenzoic acid to the polysaccharide region of LPSs, producing an off-on fluorescence (Fig. 2d, left). These functionalized microrobots were specifically designed to detect LPSs derived from *Escherichia coli* and *Salmonella enterica*^{56,57}. Quantum-dot-enhanced microrobots for LPSs from *S. enterica* were suitable for bacterial endotoxin determination in milk, mayonnaise, egg white and egg yolk samples⁵⁷ (Fig. 2d, right). LPSs from different bacteria (and even from the same species) have a common core chemical structure but differ on most external polysaccharide chains. Previous studies show that the quenching of GQD fluorescence by external polysaccharide chains indicates varying degrees of interaction with LPS, which in turn depends on the bacterial strain involved.

This variability underscores the need for precise control in the design of microrobot-based assays for LPS detection.

One of the key benefits of using microrobots is the substantial reduction in analysis times. Other advantages include low-volume samples and a user-friendly analytical process. However, gold-standard methods are regulated to ensure food security; for example, regulations require enrichment cultures and selective analysis for pathogenic organism determination. Moreover, conventional methods for detecting toxins and contaminants require costly equipment, which in some cases need special infrastructure and trained personnel, and are usually time consuming^{58–60}. Functionalized microrobots have been reported for detecting toxins such as soman simulants, *Clostridium difficile* toxin and cholera toxin B in water or biological fluid^{61–63}. Microrobots can thus act as moving sensing platforms⁶⁴.

Enhancing food preservation using microrobots

Product recalls due to food spoilage can lead to substantial economic losses^{65–67}. There is growing interest in developing and deploying microrobots for direct elimination of pathogenic microorganisms. These microrobots can be engineered to capture and remove pathogenic microorganisms from food matrices, or to sterilize food by neutralizing microorganisms without altering the food’s intrinsic properties^{68–71}. In addition, the microrobots can be retrieved from the food matrix by filtration or by applying a magnetic field.

Staphylococcus aureus poses a contamination risk through food handling. To efficiently remove *S. aureus* from food, one approach is to use GO/Pt NP/Fe₂O₃ magneto-catalytic microrobots⁶⁸. The GO from the microrobots’ surface was functionalized with nisin, an antimicrobial polypeptide sourced from lactic acid bacteria. Nisin targets the lipid II molecule, a key component in the cell membrane of *S. aureus*. This covalent attachment to GO is facilitated by the material’s versatile chemical properties. The incorporation of nisin significantly enhances the microrobots’ ability to attract *S. aureus*, increasing pathogen capture compared with the use of nisin in its free form. Moreover, these GO/Pt NP/Fe₂O₃ microrobots show high selectivity to *S. aureus*, even in environments containing other bacteria such as *E. coli*. When applied in juice samples, the antimicrobial microrobots achieved high efficiency in removing *S. aureus* within 20 minutes, using hydrogen peroxide as the propulsion agent.

A magnetic actuation method has also been introduced to manoeuvre microrobots with comparable efficiency, achieving 80% removal of *S. aureus*, representing a promising strategy for automating food processing. Magnetically actuated microrobots have been specifically engineered for the safe and efficient removal of *S. aureus* from milk, showing their adaptability and potential for enhancing food safety⁶⁹. Magnetic microrobots functionalized with fluorescence-tagged immunoglobulins (MagRobots- α IgG@IgG) have been effectively used for the targeted isolation of bacteria, leveraging their innate biorecognition of protein A on the cell walls of *S. aureus*. These MagRobots- α IgG@IgG are manoeuvred through milk using a custom-designed, 3D-printed six-coil system that generates a transversal rotating magnetic field. This system allows precise programming of the microrobots’ movement patterns, enabling them to ‘walk’ and rotate over the milk’s matrix to isolate *S. aureus* efficiently, even in the presence of competing bacteria such as *E. coli*. This magnetic system facilitates elimination of *S. aureus* after just 1 hour of treatment (60% *S. aureus* removed) without disrupting the natural milk microbiota, presenting a viable solution for large-scale industrial application. Moreover, it is well known that *S. aureus* can survive pasteurization and thermal sterilization processes, and staphylococcal enterotoxins are stable and cannot be easily eradicated by common hygienic procedures once they are formed in dairy products. Therefore, magnetic robots offer a promising alternative for the dairy industry.

Food substrates, however, are vulnerable to various foodborne pathogens beyond *S. aureus*. For example, *Listeria monocytogenes* poses a severe health threat, particularly to vulnerable populations⁷². In response to this threat, screw-shaped Fe₃O₄-spirulina magnetic

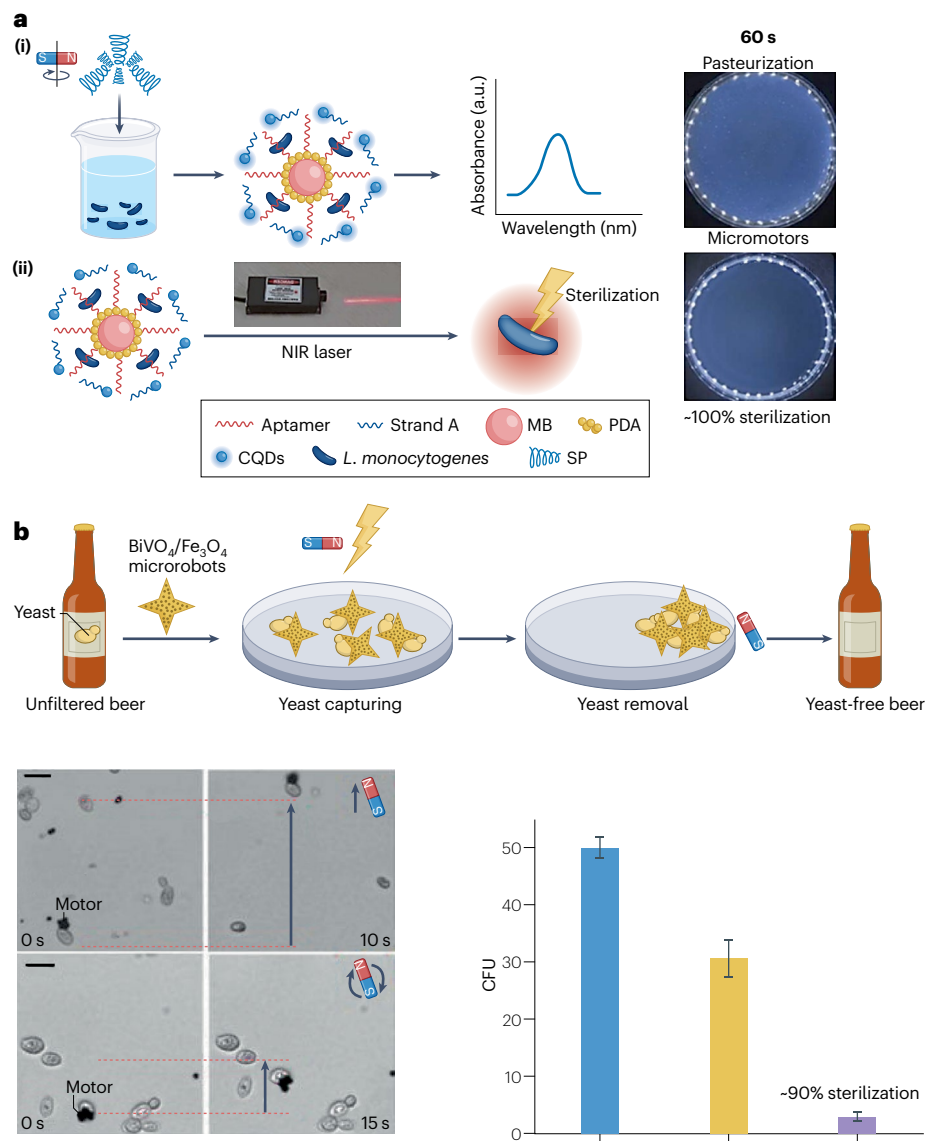


Fig. 3 | Microrobots for food preservation applications. **a**, Left: schematic representation of magnetic micromotors functionalized with specific fluorescence-tagged aptamers for *L. monocytogenes* fluorescence detection (i) and milk sample sterilization mechanism by the micromotors under NIR irradiation (ii). Right: plate comparison diagrams of sterilization effects after 60 seconds of pasteurization treatment and magnetic micromotors irradiated with NIR light. **b**, Top: improving beer-brewing processes with microrobots. The diagram shows the removal process of yeast cells by photocatalytic and

magnetic $\text{BiVO}_4/\text{Fe}_3\text{O}_4$ microrobots in real non-filtered beer samples. Bottom left: *S. cerevisiae* yeast manipulation by $\text{BiVO}_4/\text{Fe}_3\text{O}_4$ microrobots under combined light and magnetic fields in beer samples. Scale bar, 10 μm . Bottom right: colony-forming unit (CFU) values of beer in the absence of the micromotors (control) and the presence of magnetically actuated $\text{BiVO}_4/\text{Fe}_3\text{O}_4$ microrobots in the dark and under light illumination ($n = 3$; error bars represent the standard deviation). MB, magnetic beads; SP, spirulina. Panels adapted with permission from: **a**, ref. 70, Elsevier; **b**, ref. 71, Wiley.

microrobots have been engineered to detect and neutralize *L. monocytogenes* in milk samples, showcasing the adaptability of microrobot technology for different types of foodborne pathogens⁷⁰. Magnetic spirulina micromotors were covered with polydopamine (PDA) and functionalized with a specific aptamer for *L. monocytogenes* (A1) and a partial complementary aptamer tagged with CQD fluorescence tags (A2/CQDs). *L. monocytogenes* detection was based on an off-on fluorescence strategy. When A1 and A2/CQDs hybridize, the CQDs come into close proximity with PDA, resulting in fluorescence quenching. However, in the presence of *L. monocytogenes*, the A1-bacteria complex is more stable than the A1-A2/CQD duplex, leading to the release of A2/CQDs into the medium, where the restored fluorescence of CQDs becomes detectable (Fig. 3a(i)). This strategy showed great potential for monitoring *L. monocytogenes*. Moreover, these magnetic

screw-shaped micromotors can kill *L. monocytogenes* bacteria using externally applied near-infrared (NIR) irradiation. When the $\text{Fe}_3\text{O}_4@$ PDA micromotors were treated with NIR irradiation, they generated heat due to molecular vibrations, resulting in local hot points reaching 65 °C (Fig. 3a(ii)). As a result, bacteria were killed by thermotherapy via micromotors irradiated by NIR. This treatment was highly efficient compared with standard pasteurization, achieving almost 100% bacteria eradication in only 60 s (Fig. 3a, right). In addition, thermal treatment using magnetic micromotors caused less modification of the food's natural proteins than pasteurization.

Bacteria are not the only microorganisms responsible for food spoilage; for example, yeast cells used in many fermentation processes can also produce mycotoxins that poison cereal silos⁷³. However, they are inactivated or eliminated at the end of the process to avoid product

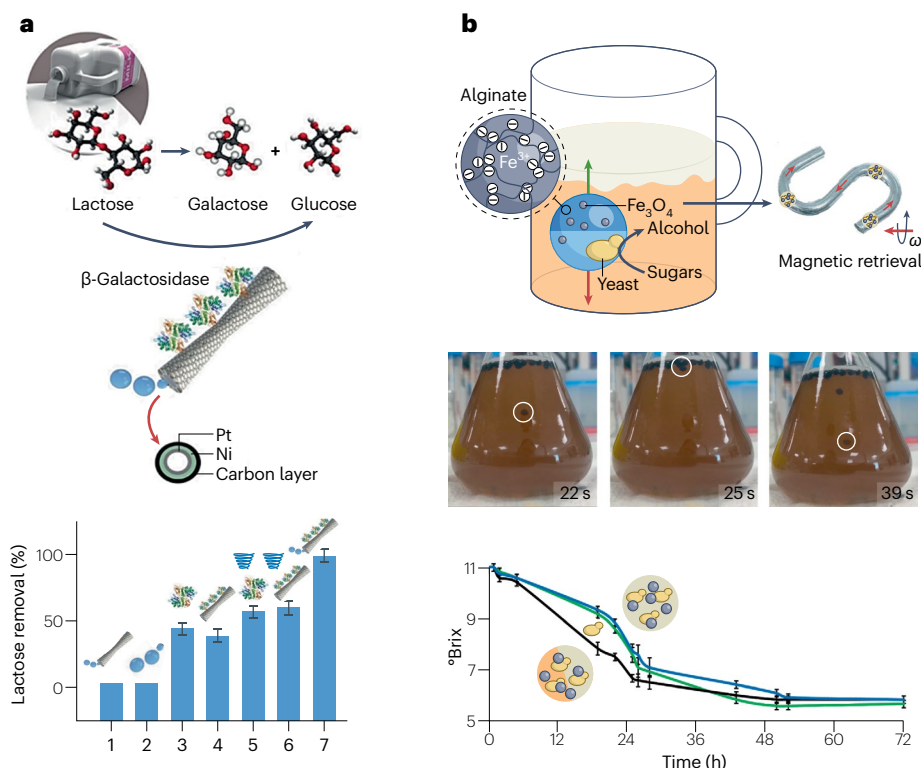


Fig. 4 | Microrobots for food-processing applications. **a**, Top: schematic representation of the β -galactosidase-based Pt microrobots' mechanism for lactose removal from milk. Bottom: lactose removal efficiency using (from left to right): (1) multiwalled-nanotube-enhanced Ni-Pt microrobots; (2) H_2O_2 ; (3) free enzyme; (4) static β -galactosidase microrobots; (5) free enzyme under mechanical stirring; and (7) swimming β -galactosidase microrobots ($n=3$; error bars represent the standard deviation). **b**, Top and middle: schematic of the oscillatory motion mechanism of spherical yeast-based BioBots during brewing, with images of the

process and their removal from the beer at the end. White circles highlight the position of a biobot. Bottom: monitoring of the brewing process expressed as °Brix (1°Brix corresponds to 1 g of sugars per 100 g of solution) using spherical Janus ALG@yeast- Fe_3O_4 (Alginate@yeast-ferrite) BioBots (black line), non-Janus floating BioBots (blue line) and free yeast (green line) ($n=3$; error bars represent the standard deviation). Panel **a** adapted with permission from ref. 76, Wiley. Panel **b** reproduced with permission from ref. 79 under a Creative Commons license CC BY 4.0.

spoilage⁷⁴. Magnetic- and light-propelled microrobots comprising $BiVO_4$ microparticles decorated with Fe_3O_4 NPs were designed for yeast cell removal from beer, using dual propulsion through visible light (enabled by the photocatalytic properties of $BiVO_4$) and magnetic fields (due to the presence of Fe_3O_4 NPs)⁷⁵. The moving microrobots captured yeast cells by physical adhesion. Moreover, their magnetic properties enabled the removal of the microrobots from the food substrate through magnetic entrapment, yielding yeast-free beer (Fig. 3b, top). The combination of light and magnetic fields for microrobot propulsion achieved a 2-fold increase in yeast cell elimination (>90% yeast cells removed) compared with only magnetically actuated microrobots (Fig. 3b, bottom). In addition, beer-treated $BiVO_4/Fe_3O_4$ microrobots showed that precipitate traces of V and Fe were within allowed limits, with no changes to the final beer properties. Thus, microrobots hold great potential for solving yeast spoilage in fermented products.

Magnetic- and light-propelled robots showed that food samples were not compromised by the presence of microrobots⁷⁶. However, there are still limitations to applying microrobots in food preservation. These robots are commonly fabricated using metallic or inorganic elements that require continuous ion-release monitoring to avoid possible contamination of the food matrix. Therefore, developing biocompatible polymeric or protein-based microrobots would help prevent heavy metal contamination from inorganic materials-based microrobots.

Food processing using microrobots

So far, only a few examples of microrobots have been used to enhance food processes. Vanillyl alcohol (VA) is a high-value food additive

produced by vanillin reduction. A pioneering work⁷⁵ described the use of $NaBH_4$ particles covered with a reduced GO composite (wax-rGO) for 'on-the-fly' VA synthesis and isolation from the reaction pot. These microrobots propelled themselves by generating H_2 bubbles from $NaBH_4$ decomposition at the water-air interface. Moreover, the wax-rGO coating served as a hydrophobic sponge for VA isolation from the surrounding medium. As a result, high-purity VA edible additive was obtained in a fast process without distillation purification steps.

Lack of lactase in the intestinal tract causes milk intolerance worldwide. Thus, the food industry has developed an enzymatic method to hydrolyse lactose to produce lactose-free milk. Tubular microrobots functionalized with hydrolytic enzymes (β -galactosidase) to convert lactose in milk into its monosaccharides have been developed⁷⁶. One of these methods uses β -galactosidase under stirring conditions. An enzymatic moving platform was prepared based on an external layer of electrodeposited multiwall carbon nanotubes to covalently attach β -galactosidase enzyme to the surface. In addition, an intermediate magnetic layer of Ni was used for microrobot removal using a static magnet for reuse in a new process. The internal catalytic layer of Pt NPs was used for microrobot bubble propulsion in milk by adding H_2O_2 fuel (Fig. 4a, top). The on-the-fly enzymatic activity of microrobots results in lactose hydrolysis in only 20–25 min. In addition, on-the-fly lactose hydrolysis performance was superior compared with mechanical stirring of free enzyme or β -galactosidase-based microrobots (Fig. 4a, bottom). Enzymatic activity was not altered after its immobilization on the surface of the carbon-based microrobots, indicating their great potential for use in different industrial enzymatic food processes. However,

while β -galactosidase-based Pt microrobots propelled themselves by H_2O_2 decomposition, additional steps were required to remove it from milk after lactose hydrolysis; hence, the fuel used for their catalytic propulsion should be replaced with biocompatible fuel or magnetic propulsion. The main approach for substituting H_2O_2 is to use highly reactive metals such as Mg, which generate H_2 bubbles in water to propel the microrobots⁷⁷.

To enhance the food fermentation process, various propulsion mechanisms have been developed for microrobot propulsion. One such approach is the buoyancy-shift mechanism, in which bubbles generated and absorbed on the microrobots' surface promote upwards vertical motion in the solution and, consequently, bubble release that promotes downwards motion⁷⁸. For beer fermentation, 'BioBots' were produced by encapsulating yeast cells into biocompatible alginate polymer beads along with Fe_3O_4 NPs⁷⁹. A continuous vertical oscillatory motion was then achieved as sugar fermentation produced CO_2 gas bubbles inside the BioBots, causing a continuous shift in their buoyancy (Fig. 4b, top). Moreover, Janus-shaped BioBots sedimented when CO_2 evolution ceased, enabling their separation from beer via magnetic actuation. As a result, it was not necessary to remove the yeast cells at the end of the process to obtain the beer. The Janus BioBots' catalytic motion improved the fermentation process by several hours compared with floating yeast or floating non-Janus BioBots (without motion) due to their intermixing capabilities (Fig. 4b, bottom).

Conclusion and future perspectives

This Review summarizes the advances in miniaturized robot technology for food safety control, preservation and processing. The primary benefits of these robots include enhanced reaction rates through on-the-fly chemistry and the potential for greater automation, thereby reducing human–food interaction. These microrobots are designed to navigate and actuate within various food substrates, improving mixing and accelerating reaction rates—particularly in more viscous media. Automation has also been advanced through the use of microrobots for efficient microorganism removal. While the technology presents promising avenues for rapid procedures and automation in food safety and preservation, it also faces several challenges. One such challenge is scalability: despite progress in mass production, the synthesis and functionalization of microrobots still lack the scalability needed for widespread food industry applications. Future research should focus on scalable methodologies to produce functional microrobots in large quantities and at low cost. In this context, millimetre-, micrometre- and even nanometre-sized robots have the upper hand owing to new technological developments, such as 3D printing, which allows scalability⁸⁰. Smaller robots can be synthesized in high quantities by chemical synthesis or physical deposition processes; however, further progress is needed to obtain complex functional robots⁸¹. There is also potential in integrating multiple functionalities into a single robot, and incorporating machine learning into microrobot navigation systems^{82,83}. Safety issues related to microrobots used on food substrates must be addressed. We believe that the potential of microrobots will encourage multidisciplinary collaborations aimed at scaling up technologies and guiding the development of new materials derived from the food substrates, rather than relying on external chemical additives. Ultimately, miniaturized robotics technology holds promise for food safety control, contaminant elimination for food preservation and the advancement of food-processing techniques.

References

- Wang, Y., Borgatta, J. & White, J. C. Protecting foods with biopolymer fibres. *Nat. Food* **3**, 402–403 (2022).
- Snyder, A. B., Martin, N. & Wiedmann, M. Microbial food spoilage: impact, causative agents and control strategies. *Nat. Rev. Microbiol.* **22**, 528–542 (2024).
- Sanders, T. A. B. Food production and food safety. *BMJ* **318**, 1689–1693 (1999).
- Camino Feltes, M. M., Arispetto-Bragotto, A. P. & Block, J. M. Food quality, food-borne diseases, and food safety in the Brazilian food industry. *Food Qual. Saf.* **1**, 13–27 (2017).
- Smith, J. L. & Fratamico, P. M. Emerging and re-emerging foodborne pathogens. *Foodborne Pathog. Dis.* **15**, 737–757 (2018).
- Bélanger, P., Tanguay, F., Hamel, M. & Phypers, M. An overview of foodborne outbreaks in Canada reported through Outbreak Summaries: 2008–2014. *Can. Commun. Dis. Rep.* **41**, 254–262 (2015).
- Crippa, M. et al. Food systems are responsible for a third of global anthropogenic GHG emissions. *Nat. Food* **2**, 198–209 (2021).
- Sarno, E., Pezzutto, D., Rossi, M., Liebana, E. & Rizzi, V. A review of significant European foodborne outbreaks in the last decade. *J. Food Prot.* **84**, 2059–2070 (2021).
- Beltran-Alcrudo, D., Falco, J. R., Raizman, E. & Dietze, K. Transboundary spread of pig diseases: the role of international trade and travel. *BMC Vet. Res.* **15**, 64 (2019).
- Vandeweyer, D., Lievens, B. & Campenhout, L. V. Identification of bacterial endospores and targeted detection of foodborne viruses in industrially reared insects for food. *Nat. Food* **1**, 511–516 (2020).
- Villalonga, A., Sánchez, A., Mayol, B., Reviejo, J. & Villalonga, R. Electrochemical biosensors for food bioprocess monitoring. *Curr. Opin. Food Sci.* **43**, 18–26 (2022).
- Nahar, S., Mizan, M. F. R., Ha, A. J.-W. & Ha, S.-D. Advances and future prospects of enzyme-based biofilm prevention approaches in the food industry. *Compr. Rev. Food Sci. Food Saf.* **17**, 1484–1502 (2018).
- Bhanja, A., Nanda, R. & Mishra, M. in *Bio- and Nano-sensing Technologies for Food Processing and Packaging* (ed. Shukla, A. K.) 181–198 (Royal Society of Chemistry, 2022); <https://doi.org/10.1039/9781839167966>
- Peters, R. J. B. et al. Nanomaterials for products and application in agriculture, feed and food. *Trends Food Sci. Technol.* **54**, 155–164 (2016).
- Dey, A., Pandey, G. & Rawtani, D. Functionalized nanomaterials driven antimicrobial food packaging: a technological advancement in food science. *Food Control* **131**, 108469 (2022).
- Chen, H. et al. Nanomaterials as optical sensors for application in rapid detection of food contaminants, quality and authenticity. *Sens. Actuators B* **329**, 129135 (2021).
- Mundaca-Uribe, R., Askarinam, N., Fang, R. H., Zhang, L. & Wang, J. Towards multifunctional robotic pills. *Nat. Biomed. Eng.* <https://doi.org/10.1038/s41551-023-01090-6> (2023).
- Nelson, B. J. & Pané, S. Delivering drugs with microrobots. *Science* **382**, 1120–1122 (2023).
- Fernández-Medina, M., Ramos-Docampo, M. A., Hovorka, O., Salgueiriño, V. & Städler, B. Recent advances in nano- and microrobots. *Adv. Funct. Mater.* **30**, 1908283 (2020).
- Allard, C. Adaptable navigation of magnetic microrobots. *Nat. Rev. Mater.* **9**, 90 (2024).
- Hu, Y., Liu, W. & Sun, Y. Self-propelled micro-/nanorobots as 'on-the-move' platforms: cleaners, sensors, and reactors. *Adv. Funct. Mater.* **32**, 2109181 (2022).
- Wang, T., Wu, Y., Yildiz, E., Kanyas, S. & Sitti, M. Clinical translation of wireless soft robotic medical devices. *Nat. Rev. Bioeng.* **2**, 470–485 (2024).
- Yuan, K., Jiang, Z., Jurado-Sánchez, B. & Escarpa, A. Nano/micro-robots for diagnosis and therapy of cancer and infectious diseases. *Chem. Eur. J.* **26**, 2309–2326 (2020).
- Esteban-Fernández de Ávila, B. et al. Microrobots go in vivo: from test tubes to live animals. *Adv. Funct. Mater.* **28**, 1705640 (2018).

25. Urso, M., Ussia, M. & Pumera, M. Smart micro- and nanorobots for water purification. *Nat. Rev. Biolog.* **1**, 236–251 (2023).
26. Ge, H., Chen, X., Liu, W., Lu, X. & Gu, Z. Metal-based transient microrobots: from principle to environmental and biomedical applications. *Chem. Asian J.* **14**, 2348–2356 (2019).
27. Dan, J. et al. Micro/nanorobot technology: the new era for food safety control. *Crit. Rev. Food Sci. Nutr.* **64**, 2032–2052 (2024).
28. Wang, Q. & Zhang, L. External power-driven microrobotic swarm: from fundamental understanding to imaging-guided delivery. *ACS Nano* **15**, 149–174 (2021).
29. Wang, H. & Pumera, M. Coordinated behaviors of artificial micro/nanomachines: from mutual interactions to interactions with the environment. *Chem. Soc. Rev.* **49**, 3211–3230 (2020).
30. Singh, V. V., Kaufmann, K., de Ávila, B. E.-F., Karshalev, E. & Wang, J. Molybdenum disulfide-based tubular microengines: toward biomedical applications. *Adv. Funct. Mater.* **26**, 6270–6278 (2016).
31. Kim, J., Mayorga-Martinez, C. C. & Pumera, M. Magnetically boosted 1D photoactive microswarm for COVID-19 face mask disruption. *Nat. Commun.* **14**, 935 (2023).
32. Chen, C., Karshalev, E., Guan, J. & Wang, J. Magnesium-based micromotors: water-powered propulsion, multifunctionality, and biomedical and environmental applications. *Small* **14**, 1704252 (2018).
33. Zhou, H., Mayorga-Martinez, C. C., Pané, S., Zhang, L. & Pumera, M. Magnetically driven micro and nanorobots. *Chem. Rev.* **121**, 4999–5041 (2021).
34. Chen, X.-Z. et al. Recent developments in magnetically driven micro- and nanorobots. *Appl. Mater. Today* **9**, 37–48 (2017).
35. Li, J. C. C., Mayorga-Martinez, C.-D., Ohl, M. & Pumera, M. Ultrasonically propelled micro- and nanorobots. *Adv. Funct. Mater.* **32**, 2102265 (2022).
36. Chen, C., Soto, F., Karshalev, E., Li, J. & Wang, J. Hybrid nanovehicles: one machine, two engines. *Adv. Funct. Mater.* **29**, 1806290 (2018).
37. Ussia, M. et al. Magnetically driven self-degrading zinc-containing cystine microrobots for treatment of prostate cancer. *Small* **19**, 2208259 (2023).
38. Song, S.-J. et al. Precisely navigated biobot swarms of bacteria *Magnetospirillum magneticum* for water decontamination. *ACS Appl. Mater. Interfaces* **15**, 7023–7029 (2023).
39. Mayorga-Martinez, C. C., Fojtů, M., Vyskočil, J., Cho, N.-J. & Pumera, M. Pollen-based magnetic microrobots are mediated by electrostatic forces to attract, manipulate, and kill cancer cells. *Adv. Funct. Mater.* **32**, 2207272 (2022).
40. Kim, J. et al. Advanced materials for micro/nanorobotics. *Chem. Soc. Rev.* **53**, 9190–9253 (2024).
41. Ussia, M. & Pumera, M. Towards micromachine intelligence: potential of polymers. *Chem. Soc. Rev.* **51**, 1558–1572 (2022).
42. Yang, K., Won, S., Park, J. E., Jeon, J. & Wie, J. J. Magnetic swarm intelligence of mass-produced, programmable microrobot assemblies for versatile task execution. *Device* **3**, 100626 (2025).
43. Wang, J. Self-propelled affinity biosensors: moving the receptor around the sample. *Biosens. Bioelectron.* **76**, 234–242 (2016).
44. Dai, B. et al. Fluid field modulation in mass transfer for efficient photocatalysis. *Adv. Sci.* **9**, 2203057 (2022).
45. Xiong, K. et al. An axis-asymmetric self-driven microrobot that can perform precession multiplying ‘on-the-fly’ mass transfer. *Matter* **6**, 907–924 (2023).
46. Karshalev, E., Esteban-Fernández de Ávila, B. & Wang, J. Microrobots for ‘chemistry-on-the-fly’. *J. Am. Chem. Soc.* **140**, 3810–3820 (2018).
47. Rojas, D., Jurado-Sánchez, B. & Escarpa, A. ‘Shoot and sense’ Janus microrobots-based strategy for the simultaneous degradation and detection of persistent organic pollutants in food and biological samples. *Anal. Chem.* **88**, 4153–4160 (2016).
48. Kong, L., Guan, J. & Pumera, M. Micro- and nanorobots based sensing and biosensing. *Curr. Opin. Electrochem.* **10**, 174–182 (2018).
49. Luo, Y. et al. MnFe₂O₄ microrobots enhanced field digestion and solid phase extraction for on-site determination of arsenic in rice and water. *Anal. Chim. Acta* **1156**, 338354 (2021).
50. Toh, S. Y., Citartan, M., Gopinath, S. C. B. & Tang, T.-H. Aptamers as a replacement for antibodies in enzyme-linked immunosorbent assay. *Biosens. Bioelectron.* **64**, 392–403 (2015).
51. Esteban-Fernandez de Ávila, B. et al. Aptamer-modified graphene-based catalytic microrobots: off-on fluorescent detection of ricin. *ACS Sens.* **1**, 217–221 (2016).
52. Molinero-Fernandez, A., Jodra, A., Moreno-Guzman, M., Lopez, M. A. & Escarpa, A. Magnetic reduced graphene oxide/nickel/platinum nanoparticles microrobots for mycotoxin analysis. *Chem. Eur. J.* **24**, 7172–7176 (2018).
53. Maria-Hormigos, R., Jurado-Sánchez, B. & Escarpa, A. Carbon allotrope nanomaterials based catalytic microrobots. *Chem. Mater.* **28**, 8962–8970 (2016).
54. Molinero-Fernandez, A., Moreno-Guzman, M., Lopez, M. A. & Escarpa, A. Biosensing strategy for simultaneous and accurate quantitative analysis of mycotoxins in food samples using unmodified graphene microrobots. *Anal. Chem.* **89**, 10850–10857 (2017).
55. Wen, J., Xu, Y., Li, H., Lu, A. & Sun, S. Recent applications of carbon nanomaterials in fluorescence biosensing and bioimaging. *Chem. Commun.* **51**, 11346–11358 (2015).
56. Jurado-Sánchez, B., Pacheco, M., Rojo, J. & Escarpa, A. Magnetocatalytic graphene quantum dots Janus microrobots for bacterial endotoxin detection. *Angew. Chem. Int. Ed.* **56**, 6957–6961 (2017).
57. Pacheco, M., Jurado-Sánchez, B. & Escarpa, A. Sensitive monitoring of enterobacterial contamination of food using self-propelled Janus microsensors. *Anal. Chem.* **90**, 2912–2917 (2018).
58. Su, W. & Ding, X. Methods of endotoxin detection. *J. Lab. Autom.* **20**, 354–364 (2015).
59. Sorbo, A. et al. Food safety assessment: overview of metrological issues and regulatory aspects in the European Union. *Separations* **9**, 53 (2022).
60. Romero-González, R. Food safety: how analytical chemists ensure it. *Anal. Methods* **7**, 7193–7201 (2015).
61. Singh, V. V. et al. Micromotor-based on-off fluorescence detection of sarin and soman simulants. *Chem. Commun.* **51**, 11190–11193 (2015).
62. Zhang, Y. et al. Real-time tracking of fluorescent magnetic spore-based microrobots for remote detection of *C. diff* toxins. *Sci. Adv.* **5**, eaau9650 (2019).
63. Yuan, K., López, M. Á., Jurado-Sánchez, B. & Escarpa, A. Janus micromotors coated with 2d nanomaterials as dynamic interfaces for (bio)-sensing. *ACS Appl. Mater. Interfaces* **12**, 46588–46597 (2020).
64. Mayorga-Martinez, C. C. & Pumera, M. Self-propelled tags for protein detection. *Adv. Funct. Mater.* **30**, 1906449 (2020).
65. Turgis, M., Vu, K. D., Dupont, C. & Lacroix, M. Combined antimicrobial effect of essential oils and bacteriocins against foodborne pathogens and food spoilage bacteria. *Food Res. Int.* **48**, 696–702 (2012).
66. Heymich, M.-L. et al. Generation of antimicrobial peptides Leg1 and Leg2 from chickpea storage protein, active against food spoilage bacteria and foodborne pathogens. *Food Chem.* **347**, 128917 (2021).
67. Fidan, H. et al. Recent developments of lactic acid bacteria and their metabolites on foodborne pathogens and spoilage bacteria: facts and gaps. *Food Biosci.* **47**, 101741 (2022).

68. Yuan, K., Jurado-Sánchez, B. & Escarpa, A. Dual-propelled lanbiotic based Janus microrobots for selective inactivation of bacteria biofilms. *Angew. Chem. Int. Ed.* **60**, 4915–4924 (2021).
69. Mayorga-Martinez, C. C., Castoralova, M., Zelenka, J., Rumí, T. & Pumera, M. Swarming magnetic microrobots for pathogen isolation from milk. *Small* <https://doi.org/10.1002/smll.202205047> (2023).
70. Sun, F., Yao, M., Su, H., Yang, Q. & Wu, W. A magnetic fluorescent spirochetes microrobot: dynamic monitoring and in situ sterilization of foodborne pathogens. *Sens. Actuators B.* **385**, 133679 (2023).
71. Villa, K., Vyskocil, J., Ying, Y., Zelenka, J. & Pumera, M. Microrobots in brewery: dual magnetic/light-powered hybrid microrobots for preventing microbial contamination in beer. *Chem. Eur. J.* **26**, 3039–3043 (2020).
72. Herrador, Z., Gherasim, A., López-Vélez, R. & Benito, A. Listeriosis in Spain based on hospitalisation records, 1997 to 2015: need for greater awareness. *Eur. Surveill.* **24**, 1800271 (2019).
73. Alonso, V. A. et al. Fungi and mycotoxins in silage: an overview. *J. Appl. Microbiol.* **115**, 637–643 (2013).
74. Suiker, I. M. & Wösten, H. A. B. Spoilage yeasts in beer and beer products. *Curr. Opin. Food Sci.* **44**, 100815 (2022).
75. Srivastava, S. K. & Schmidt, O. G. Autonomously propelled robots for value-added product synthesis and purification. *Chem. Eur. J.* **22**, 9072–9076 (2016).
76. Maria-Hormigos, R., Jurado-Sánchez, B. & Escarpa, A. Surfactant-free β-galactosidase microrobots for ‘on-the-move’ lactose hydrolysis. *Adv. Funct. Mater.* **28**, 1704256 (2018).
77. Mou, F. et al. Self-propelled microrobots driven by the magnesium–water reaction and their hemolytic properties. *Angew. Chem. Int. Ed.* **52**, 7208–7212 (2013).
78. Wu, M., Koizumi, Y., Nishiyama, H., Tomita, I. & Inagi, S. Buoyant force-induced continuous floating and sinking of Janus microrobots. *RSC Adv.* **8**, 33331–33337 (2018).
79. Maria-Hormigos, R., Mayorga-Martinez, C. C., Kincl, T. & Pumera, M. Nanostructured hybrid BioBots for beer brewing. *ACS Nano* **17**, 7595–7603 (2023).
80. Dabbagh, S. R. et al. 3D-printed microrobots from design to translation. *Nat. Commun.* **13**, 5875 (2022).
81. Sharan, P., Nsamela, A., Lesher-Pérez, S. C. & Simmchen, J. Microfluidics for microswimmers: engineering novel swimmers and constructing swimming lanes on the microscale, a tutorial review. *Small* **17**, 2007403 (2021).
82. Ju, X. et al. Technology roadmap of micro/nanorobots. *ACS Nano* <https://doi.org/10.1021/acsnano.5c03911> (2025).
83. Abbasi, S. A., et al. Autonomous 3D positional control of a magnetic microrobot using reinforcement learning. *Nat. Mach. Intell.* **6**, 92–105 (2024).

Acknowledgements

M.P. acknowledges the financial support of the ERDF/ESF project TECHSCALE (no. CZ.02.01.01/00/22_008/0004587). C.C.M.-M. was co-funded by the European Union under the REFRESH – Research Excellence For REgion Sustainability and High-tech Industries project number CZ.10.03.01/00/22_003/0000048 via the Operational Programme Just Transition. R.M.-H. thanks the Czech Science Foundation (GAČR) for funding project number 22-04132I.

Author contributions

All authors contributed to the writing of the paper. All authors have approved the final version of the paper. M.P. originated the idea of the paper and provided direction. R.M.-H. wrote the initial draft, with help from other co-authors. C.C.M.-M. and M.P. redesigned the original draft.

Competing interests

The authors declare no competing interests.

Additional information

Correspondence and requests for materials should be addressed to Martin Pumera.

Peer review information *Nature Food* thanks Chang Chen, Michael Chen, Bing Han and Wentao Zhang for their contribution to the peer review of this work.

Reprints and permissions information is available at www.nature.com/reprints.

Publisher's note Springer Nature remains neutral with regard to jurisdictional claims in published maps and institutional affiliations.

Springer Nature or its licensor (e.g. a society or other partner) holds exclusive rights to this article under a publishing agreement with the author(s) or other rightsholder(s); author self-archiving of the accepted manuscript version of this article is solely governed by the terms of such publishing agreement and applicable law.

© Springer Nature Limited 2025